FUZZY CONTROL AND OPTIMIZATION OF A PHOTOVOLTAIC SYSTEM FOR SMART BUILDING WITH LOW ENERGY CONSUMPTION

Abdelaali ALIBI[1], Larbi CHRIFI-ALAOUI[2], Sami LABDAI[3], Said DRID[4]

This paper deals with the integration of a photovoltaic energy conversion system (PVECS) into a distribution network and cater for the energy needs of buildings. The main goals of this work are the reduction of the grid dependence, minimization of the energy cost and increasing the autonomy of the building's energy. Two stages converters are used to ensure the maximum power point tracking (MPPT) and to control the power flow. A fuzzy MPPT control is proposed to maintain the power of the Photovoltaic panel at its optimal value despite climatic condition variations and building's load changes. The grid side inverter is controlled by hysteresis regulators to transfer the total produced energy, with the aim to partially or completely replace energy provided from the Grid. The DC link voltage is also stabilized in order to improve the energy quality. The complete PVECS system is modelled and simulated in Matlab/Simulink, the controllers used are simple to implement and the simulation results show that the building's energy demand can be satisfied, and the energy exceed is injected into the grid. The results confirm the good effectiveness of the proposed control.

Keywords: MPPT, Photovoltaic system, Fuzzy logic, Renewable energy, Smart building, Low consumption energy

1. Introduction

In 1998, the industrialized countries have signed the Kyoto Protocol to significantly reduce energy consumption and gas emissions while favoring the use of renewable energies. The law 2010/31/EU of May 19, 2010 on the building energy performance provides that by December 31, 2020, all new buildings will have almost zero energy consumption with anticipation for new occupied buildings and owned by the public authorities on December 31, 2018. In addition, the consumption of fossil energy decreases with the amount of renewable energy produced at these buildings [1].

[1] PHD Student, Laboratory LSPIE, Electrical Engineering department, University Batna 2, Algeria, e-mail: a.alibi@univ-batna2.dz
[2] Prof, University of Picardie Jules Verne, IUT of Cuffies, France, e-mail: larbi.alaoui@u-picardie.fr
[3] PHD Student, National Polytechnic School of Algiers, Algeria, e-mail: Sami.labdai@gmail.com
[4] Prof., Dept of Electrical Engineering, University Batna 2, Algeria, e-mail: saiddrid@ieee.org

Sustainable buildings will have to be more efficient than their current levels, and they will have to take advantage of renewable energies to approach very low energy consumption. In fact, the buildings are responsible in the world of 40% of final energy consumption, 25% of CO_2 emissions and around 30% of waste production. In this context, the building appears to be a privileged area of intervention and the integration of renewable energies and their connection to the grid is a booming solution that leads to new prospects [2].

The so-called "low- consumption building" is a complex system that can be described as a "micro-grid", where energy flows must be managed according to the demand. We are thus talking about “Smart Grid” and “Smart Building”, load shedding, power demand limitation, load curves, better integration of renewable electricity production.

Modeling energy consumption to anticipate peaks demand, according to weather prediction, makes it possible to better manage buildings and grid power [3]. This allows us to dynamically adjust power demand to the available energy, without damaging the consumer’s comfort. In particular, the installation of new generation sensors in buildings and distribution networks will provides real-time information to their managers on the various events occurring on the network. This will form a database that combines several key factors for energy management and optimization [3,4].

The idea is to make the building a gathering of decentralized production of green energy (solar, wind, superficial geothermal, biomass ...etc.). The building provides its own energy needs; the excess is injected into the grid. This kind of buildings produce more energy than they consume. This concept is called positive energy building. In general, this building can be equipped by photovoltaic systems, solar thermal collectors for heating and small wind turbines as shown in Fig. 1. In this context, photovoltaic systems offer competitive solutions with more advantages such as the absence of all pollution and the availability of sunlight most parts of the world.

In literature, we find many works on the photovoltaic energy conversion system supplying an isolated load [5-7], charging batteries [8,9], connected with the grid [9,10,11], or as renewable energy source in a smart grid [3]. The PVECS is affected by climatic conditions (temperature and irradiation) and even shading. Thus, the need for a stage of adaptation like a buck [12] or boost [9] converter to extract the maximum power from the panels.

Many algorithms were proposed and tested like incremental method in [5,12], P&O method in [12], sliding mode method in [7]. These classical methods are simple to implement; they tend to give good results but put a stress on the continuous computing of the duty cycle. It is hard to have a stable steady state with these algorithms due to the oscillations they present.

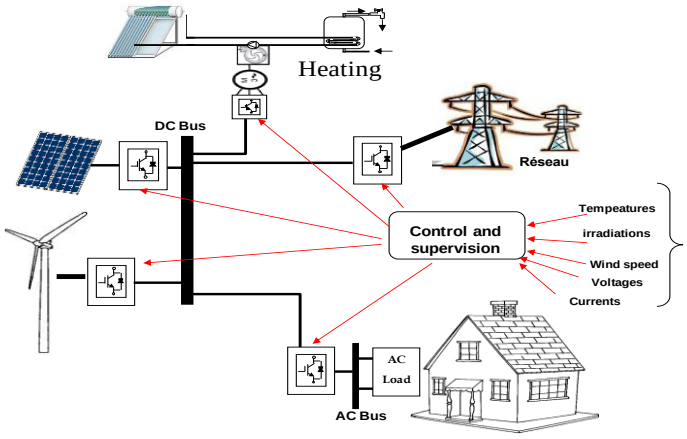

Fig.1. Integration of renewable Energy in the buildings

In [12], the authors used a PVS with a buck converter with the batteries. A comparison between incremental conductance, P&O and fuzzy MPPT technics were presented. Simulation results show the superiority of the fuzzy MPPT method against the rapid climatic changes. However, their work was not extended to the grid power injection.

In [13], the Authors try the connection of the PVECS to the grid, they used a boost chopper, they proposed an adaptive fuzzy logic controller to maximize the extracted power (MPPT). The DC-link and the synchronization were guaranteed by the conventional PI controller, their simulation results show the good reference tracking of direct and quadratic current. Nevertheless, the effects of external AC-loads on the grid have not been examined in this paper.

In this work, we focus on a Photovoltaic system (PVS) connected to both distribution grid and supplying AC loads (building). Due to the intermittent nature of sunlight and variations in loads, the output power of photovoltaic panels must be optimized. For this, we have developed a fuzzy MPPT algorithm for the DC-DC stage converter.

This study also involves applying a command to the DC-AC converter to efficiently transfer the totality of the electrical energy to the grid side with a unity power factor and optimal efficiency despite the unavoidable climatic and load perturbations.

The remainder of this paper is divided into seven main sections. We will present the general structure of the PVECS in section 2. Next, in the third section we give the mathematical model of each element of the system. In section 4 we devolved a fuzzy MPPT algorithm with the boost chopper. In section 5, we present the second adaptation stage, and we design the power flow to the grid and the loads. The Simulation results of different operating modes are illustrated in section 6. At last, we give a conclusion.

2. Structure of the Photovoltaic System

The connection of photovoltaic systems and distributed energy production sources to the grid is carried out through different topologies, we can see this in detail given by [3,14,15].

The considered system is composed of a photovoltaic generator associated to a DC/DC adaptation stage to optimally track the maximum power point. This system can supply a three-phase load and inject the exceed of power to the grid via a three-phase inverter as shown in Fig. 2. Our objectives are to fully transfer the generated power by the PV and reduce the stress on the grid.

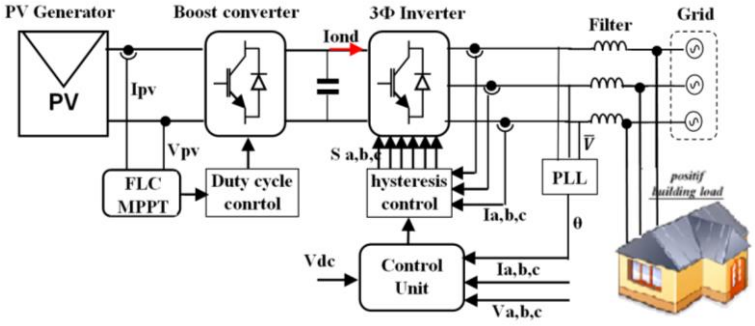

Fig.2. Block diagram of the photovoltaic energy conversion system.

3. Photovoltaic system modeling

3.1. Photovoltaic generator

A photovoltaic generator is a combination of several photovoltaic cells in series and/or in parallel in order to increase the power and the electrical voltage in accordance with the load to be supplied.

Fig. 3 shows the simplified equivalent diagram of a photovoltaic cell.

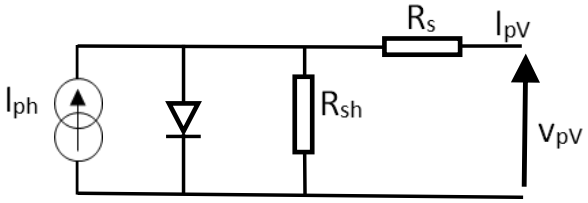

Fig.3. Equivalent circuit of photovoltaic cell

This diagram allows us to model the photovoltaic cell. The relation between the Ipv current and the Vpv generator voltage is given by Equation 1:

$$I_{pv} = I_{ph} - I_{sat}.\,exp\left[\left(\frac{e\left(V_{pv}+\left(I_{pv}*R_s\right)\right)}{nKT}\right) - 1\right] - \frac{V_{pv}+(I_{pv}*R_s)}{R_{sh}} \qquad (1)$$

where I_{sat} is the reverse saturation current, K is the Boltzmann's constant, T is the absolute temperature, e is the elementary charge, n is the ideality factor,

R_s series resistor, R_{sh} parallel resistor, I_{ph} is the photonic current,V_{pv} is the voltage across the output terminals and I_{pv} is the output current.

Considering a generator made up of Np parallel cell strings formed of Ns cells in series and that R_{sh} is infinite Equation .1 becomes:

$$I_{pv} = N_p * I_{ph} - N_p * I_{sat}.exp\left[\left(\frac{e\left(V_{pv}+\left(I_{pv}*\frac{N_p}{N_s}R_s\right)\right)}{nKT}\right) - 1\right] \quad (2)$$

The electrical parameters of the manufacturer of the BP-SX150 model photovoltaic panel used in our study are summarized in the Table 1 [16]:

Table1

BP SX150 Panel Electrical Parameters.

Description	Value
Maximum power	150 W
Voltage at p max (Vmp)	34 .5V
Current at p max (Imp)	4.35A
Open circuit volt (Voc)	43.5V
Short circuit current (Isc)	4.75A
Temperature coefficient of Isc	0.065±0.015% /Co
Temperature Coefficient of Voc	-160±20mV/ Co
Temperature Coefficient of power	-0.5±0.05% / Co
NOCT	47 ±2Co

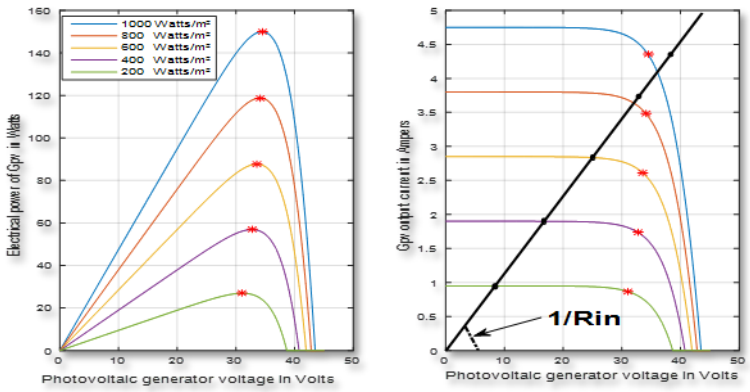

Fig. 4. *Pv-Vpv* and *Ipv-Vpv* Characteristics

The current-voltage characteristics and the power curve as a function of the voltage of the BP SX150 photovoltaic module [16] of 150 W are given by the curves of Fig. 4.

The operating point of the photovoltaic panel is defined by the load applied to its terminals, it can be different from the optimal power point. This may

depend on variation of climatic parameters (irradiation and temperature) or the load itself. Thus, the need of an electronic adapter stage to guarantee the extraction of maximal power from the photovoltaic panel.

3.2. Modelling of the DC/DC converter (Boost chopper)

The adaptation stage consists of one or more converters (boost in our study), it is introduced between the load and the photovoltaic generator. It has two main important roles, it allows the implementation of different algorithms for tracking the point of maximum electrical power of the PV generator, also it adapts the voltage level between the load and the photovoltaic generator.

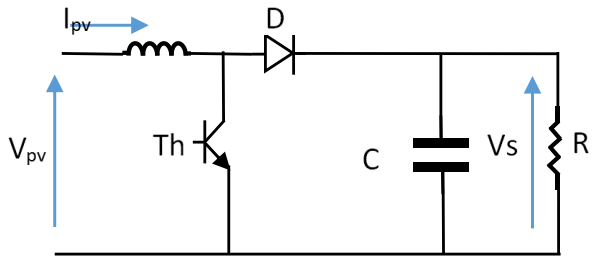

Fig. 5. Boost electrical circuit

The boost chopper, is represented by the basic electrical circuit in Fig. 5. In continuous conduction the average mathematical model of the boost converter is given by the following system of equations [15]:

$$\begin{cases} L\frac{dI_{pv}}{dt} = V_{pv} - (1-\alpha)V_s \\ C\frac{dV_s}{dt} = (1-\alpha)I_{pv} - \frac{V_s}{R} \end{cases} \quad (3)$$

where α: is the duty cycle.

From equation (3), we can see that in the steady state the relation between input output voltages and currents, are given by:

$$\begin{cases} Vs = 1/(1-\alpha)Vpv \\ I_s = (1-\alpha)I_{pv} \end{cases} \quad (4)$$

By adjusting the input impedance R_{in} of both converter and load seen by the photovoltaic panel, the duty cycle α acts to bringing back the operating point to the maximum of the power curve as represented in Fig. 4 (b).

The input impedance represents the reverse slope of the connected load. For a resistive case, R_{in} and R_{opt} value that corresponds to the Maximum power point (MPP) [17] are given by:

$$\begin{cases} R_{in} = \frac{V_{pv}}{I_{pv}} = (1-\alpha)^2 R_{ch} \\ Ropt = \frac{Vopt}{Iopt} \end{cases} \quad (5)$$

4. Maximum power point tracking algorithms

There are several operating principles for more or less efficient MPPT commands based on the properties of the PV cell. The most commonly known methods are Perturb & Observe (P&O), Hill Climbing, and Incremental Conductance (IncCond). To better understand the performance of the maximum power point tracking algorithm with the photovoltaic generators, we will briefly remind the principle through the incremental conductance method.

4.1. Incremental conductance method (IncCond)

This technique is based on the derivative of PV power by its voltage [18]. When the power derivative is zero, this means that we are on the MPP of the power curve as shown in Fig. 6.

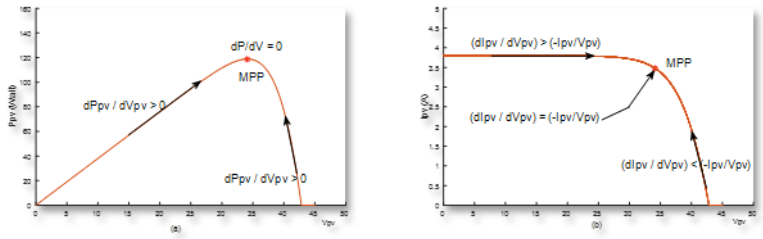

Fig. 6. Positioning the operating point based on the PV power derivative

At the MPP the following equation is verified:

$$\frac{dP_{pv}}{dV_{pv}} = \frac{d(I_{pv} * V_{pv})}{dV_{pv}} = I_{pv} + V_{pv}\frac{dI_{pv}}{dV_{pv}} = 0 \quad (6)$$

We can also write:

$$-\frac{I_{pv}}{V_{pv}} = \frac{dI_{pv}}{dV_{pv}} \quad (7)$$

We note that the left side of the equation (7) represents the conductance of the PV generator and that the right side is the incremental of this conductance.

We can locate the operating point of the PV at all-time just by comparing the conductance value with the incremental conductance. From curve of PV power in Fig. 6, the MPP is then located using the following relations [18]:

If $\frac{dI_{pv}}{dV_{pv}} > -\frac{I_{pv}}{V_{pv}}$ the operating point is left of MPP. (8a)

If $\frac{dI_{pv}}{dV_{pv}} = -\frac{I_{pv}}{V_{pv}}$ the operating point is on the MPP. (8b)

If $\frac{dI_{pv}}{dV_{pv}} < -\frac{I_{pv}}{V_{pv}}$ the operating point is right of MPP. (8c)

To track the MPP we choose the direction of the control according to the inequalities (8a) or (8c) such that the operating point reach the MPP where the equation (8b) is satisfied.

Despite the simplicity of implementation of this method, there is not a precise technic to choose the incremental step size. When it is small it results a slow tracking, on the other hand, as we increase the increment step size, the control becomes very sensible to climatic changes, this leads to a permanent oscillation around the MPP. That's why we propose the use of a fuzzy method.

4.2. Fuzzy Logic MPPT Controller

Recently, fuzzy logic control (FLC) has proven to be effective in assuring the MPPT without requiring an exact mathematical model of the system [15,19]. The fuzzy controller changes the incremental step size and direction based on the knowledge of the system behavior through a base of rules implemented in the FLC.

The structure of the fuzzy controller is given by the functional diagram in Fig. 7:

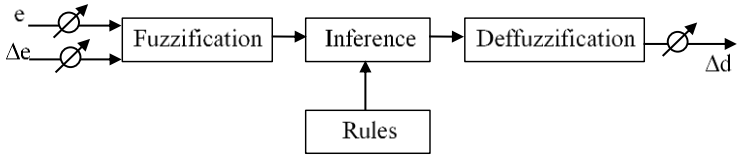

Fig.7. Structure of a fuzzy logic controller.

In our study we will use an FLC type MAMDANI with two inputs and one output. We note the first input E and its derivative ΔE the second input. The output variable Δd is the increment of the duty cycle. They are given by:

$$E = \frac{P_{(k)} - P_{(k-1)}}{V_{(k)} - V_{(k-1)}} \quad (9a)$$

$$\Delta E = E_{(k)} - E_{(k-1)} \quad (9b)$$

The fuzzification process consists in converting numerical variables into linguistic variables [10]. Each input and output can take different degrees of membership, depending on the type of membership functions, as illustrates Fig..8.

where the five membership functions are noted:

- NB : Negative Big, - NS : Negative Small,
- ZE : Zero,
- PS : Positive Small, - PB : Positive Big.

The output of the controller Δd is determined according to the fuzzy rules and the chosen inference model. In our case MAMDANI which consists of using the MIN for the AND operation then the SUM for the OR operation.

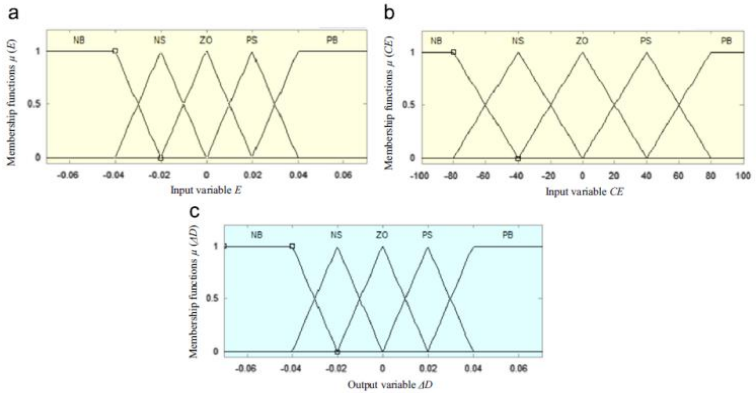

Fig. 8. Linguistiques variables : $E, \Delta E$ *and* α

In table 2, we summarize the chosen fuzzy rules.

Table 2

Table of fuzzy rules

E \ ΔE	NB	NS	ZE	PS	PB
NB	PB	PB	PB	PS	ZE
NS	PB	PB	PS	ZE	NS
ZE	PB	PS	ZE	NS	NB
PS	PS	ZE	NS	NB	NB
PB	ZE	NS	NB	NB	NB

Finally, the linguistic value of the output must be converted into a numerical value by the diffuzzification process. We will use the center of gravity method [19].

$$\Delta d = \frac{\sum_{i=1}^{n} u_i \, mf_i}{\sum_{i=1}^{n} u_i} \tag{10}$$

4.3. Simulation test results of the fuzzy MPPT

In our study, we put the fuzzy MPPT controller to test against variation of the solar irradiation and changes in load, as shown in Fig. 9.

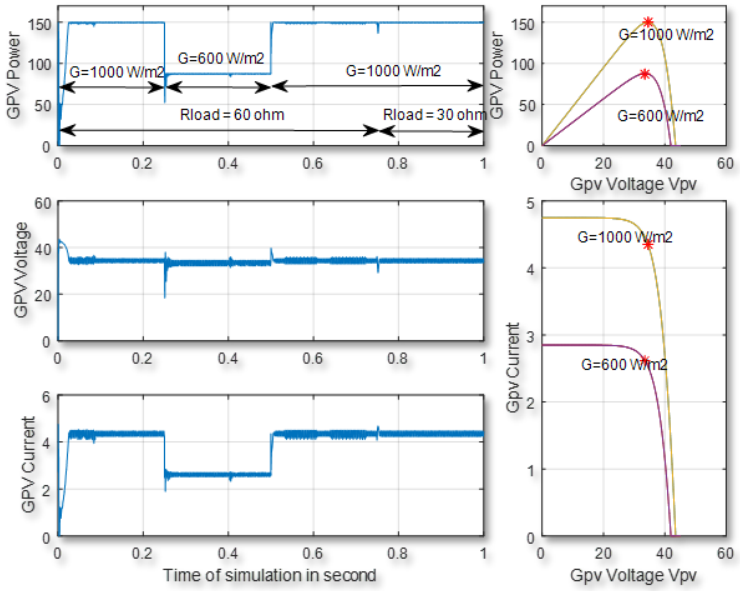

Fig. 9. Test of Fuzzy MPPT controller

From these results we can see that operation point is optimal (at the MPP) all simulation time according to the change of irradiation G from t = 0.25s to at t = 0.5s. Similarly, the PVS always operates at its MPP when we apply a variation to the load at t = 0.75s with the same weather conditions. To compare the performances of the classical MPPT algorithm (IncCond) and the fuzzy logic MPPT, the simulations were performed under exactly the same climatic conditions and with the same load profile.

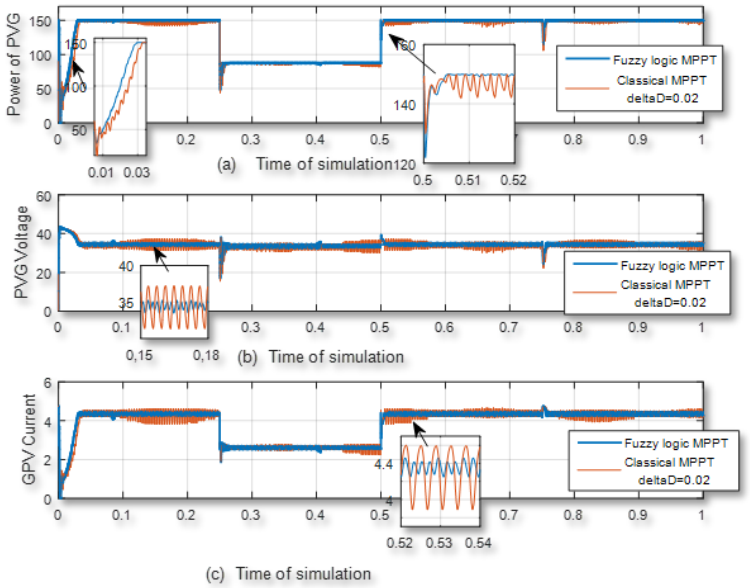

Fig. 10. Comparison of MPPT technics

In Fig. 10, it's clearly shown that the minimum start time to reach the MPP in the case of classical method is longer than in the case of Fuzzy logic MPPT. This because it is inversely depending on the duty cycle step Δd. We can see also that the PVS current, voltage, and power curves with fuzzy logic controller method are more stable and have less oscillations compare to IncCond method.

5. Grid side converter control

In the PVS, the three-phase inverter ensures that the energy produced by the PVS is transformed to AC power, so it can be injected to the grid and supply the AC loads. The overall diagram of the grid side converter control is shown in Fig..11.

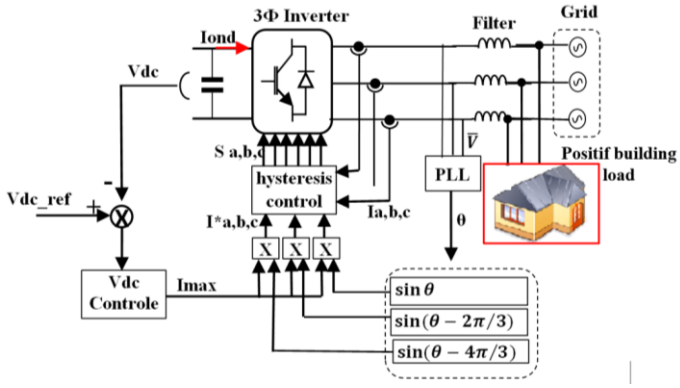

Fig. 11. Grid side converter control diagram

5.1. Power Transfer Control

The control strategy aims in the grid side converter is to transfer all the electrical energy generated in the PVECS to the building and to the grid by controlling the energy balance exchange at the DC link. The regulated current I_{ond} defines the amplitude of the reference currents (I_{max}) of the inverter. Then they have to be synchronized with the grid frequency obtained from the PLL regulator. The relationship between controlled current I_{ond} and the amplitude of references currents is given by equation (11):

$$I_{max} = \frac{\sqrt{2}\, V_{dcref}}{3\, V_s}\, I_{ond} \tag{11}$$

The inverter is modeled by the following system [18]:

$$\begin{bmatrix} V_a \\ V_b \\ V_c \end{bmatrix} = \frac{V_{dc}}{3} \begin{bmatrix} 2 & -1 & -1 \\ -1 & 2 & -1 \\ -1 & -1 & 2 \end{bmatrix} \times \begin{bmatrix} S_a \\ S_b \\ S_c \end{bmatrix} \tag{12}$$

The hysteresis regulators compare the synchronized currents (the references) with those measured from the grid side to generate the switching signals (Sa, Sb and Sc) for the inverter.

5.2 Phase locked loop (PLL)

In order to have a smooth exchange of energy with the grid, the inverter voltages must be synchronized with the frequency of the grid. For this purpose, we use phase lock loop (PLL) to detect the grid voltage frequency, then we generate the synchronized reference currents of the inverter [21].

The voltages measured at the connecting point are expressed in the bi-phase frame (α, β) by Eq. (13).

$$\begin{bmatrix} V_{s\alpha} \\ V_{s\beta} \end{bmatrix} = \sqrt{2} V_{seff} \begin{bmatrix} sin\theta \\ cos\theta \end{bmatrix} \tag{13}$$

Using the Park transformation based on the estimated angle $\hat{\theta}$, we change to the synchronism frame then we get:

$$\begin{bmatrix} V_{sd} \\ V_{sq} \end{bmatrix} = \sqrt{3} V_{seff} \begin{bmatrix} \sin(\theta - \hat{\theta}) \\ -\cos(\theta - \hat{\theta}) \end{bmatrix} \tag{14}$$

For a small difference frequency $(\theta - \hat{\theta})$ the following relationship is verified [21]:

$$V_{sd} = \sqrt{3} V_{seff} (\theta - \hat{\theta}) \tag{15}$$

When $(\theta - \hat{\theta})$ is sufficiently small we can say that $V_d = 0$. It is then possible to control θ by regulating V_d to zero as summarized in the block diagram of Fig. 12.

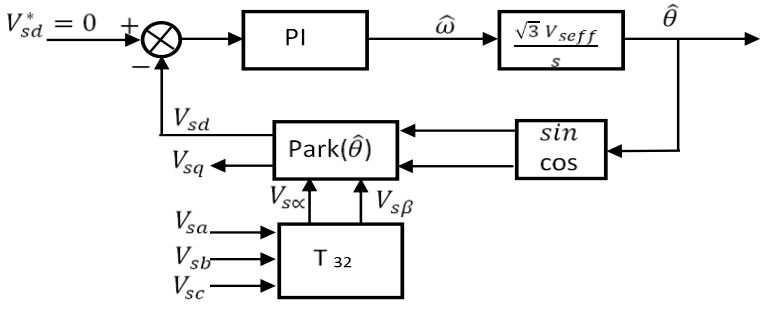

Fig. 12. The bloc scheme of the PLL

5.3 DC link controller

It is important to note that any disturbance in the energy accumulated in the DC link results a significant variation in the Vdc voltage. We seek to transfer

the totality of PVECS power to the grid side converter with minimum power loss in the DC link. The control strategy here is to create an equilibrium transfer between the power of the PVECS and the power transmitted to the grid side. The dynamic equation of the voltage Vdc is given by equation (16), [22].

$$\frac{dV_{dc}}{dt} = \frac{1}{C}(I_{pv} - I_{ond}) \tag{16}$$

The DC link voltage regulation loop is given by the diagram in Fig. 13.

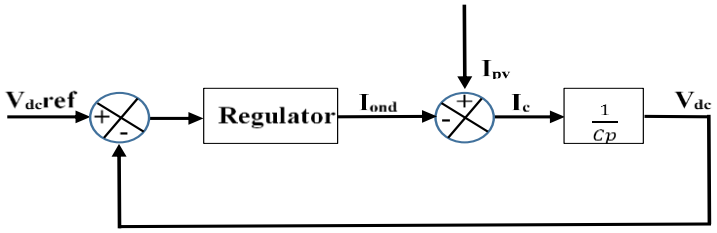

Fig. 13. Vdc voltage control loop

6. Simulation results

The overall system shown in Fig. 2 is simulated using Matlab/Simulink with the proposed fuzzy MPPT and synchronization controllers. The PV generator used is combined from series/parallel panels to produce nearly 5.4 kW.

We test our control strategy under the following conditions:

- The supplied load has a varying demand from 8 kW to 3 kW after 0.5 s of simulation time.
- A decrease of irradiation from 1000 W/m² to 600 W/m² between 0.5s to 1s.

We illustrate the load and the irradiation profiles in Fig. 14. The simulation system responses are shown in Figs. 15-19.

Fig .14. Climatic and load profile.

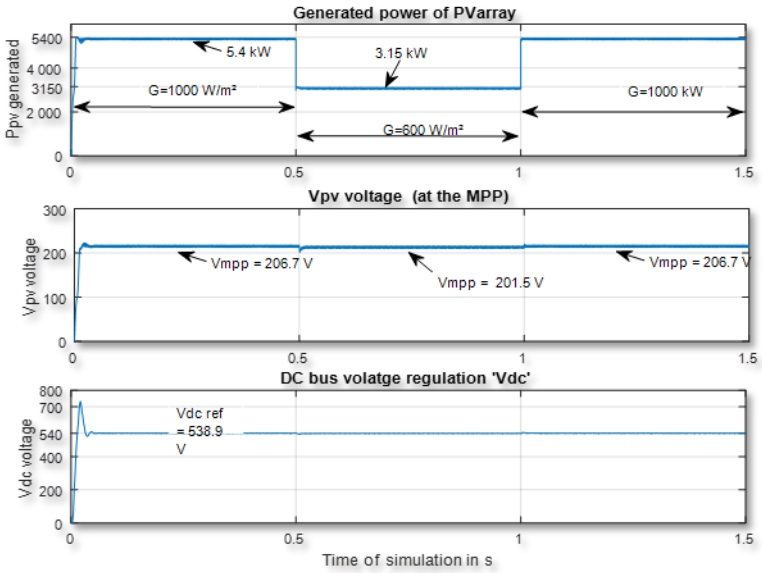

Fig. 15. (a) PV Power generated, (b) PV Voltage and (c) Vdc regulation.

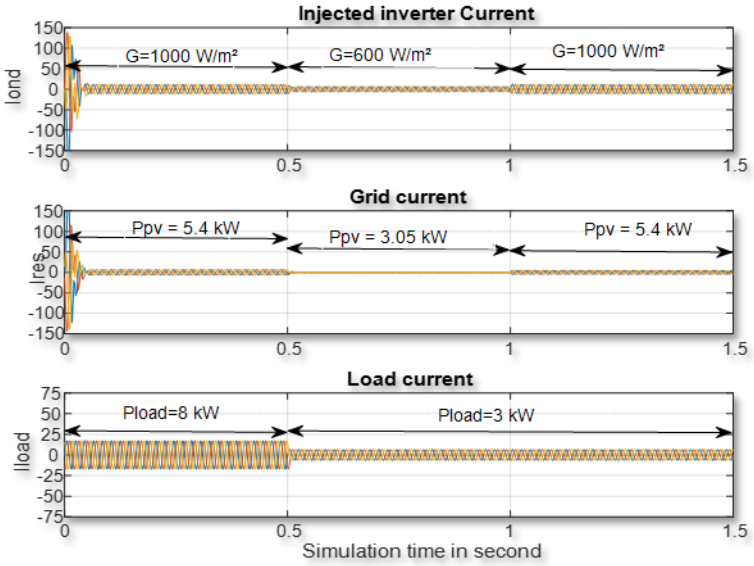

Fig. 16. Currents of the system.

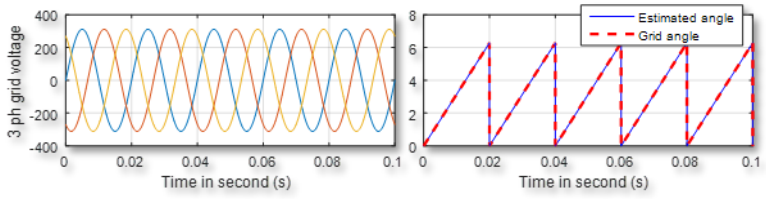

Fig.17. PLL results.

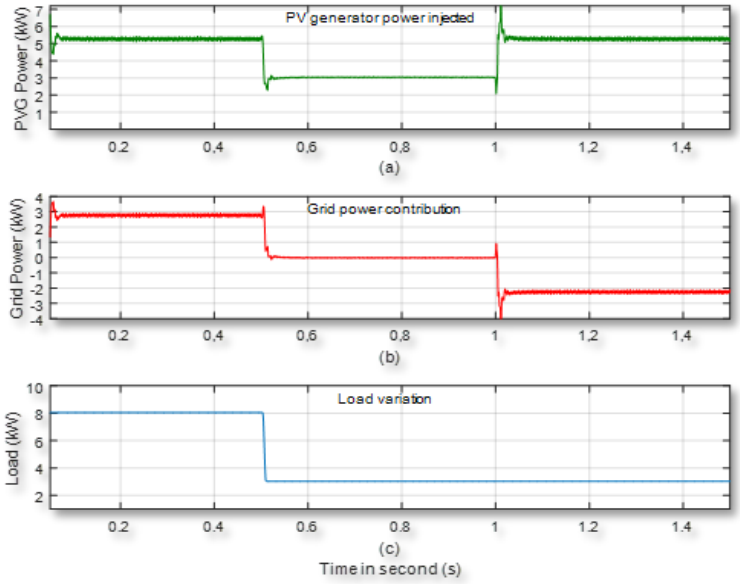

Fig .18. Power flow in the PVS

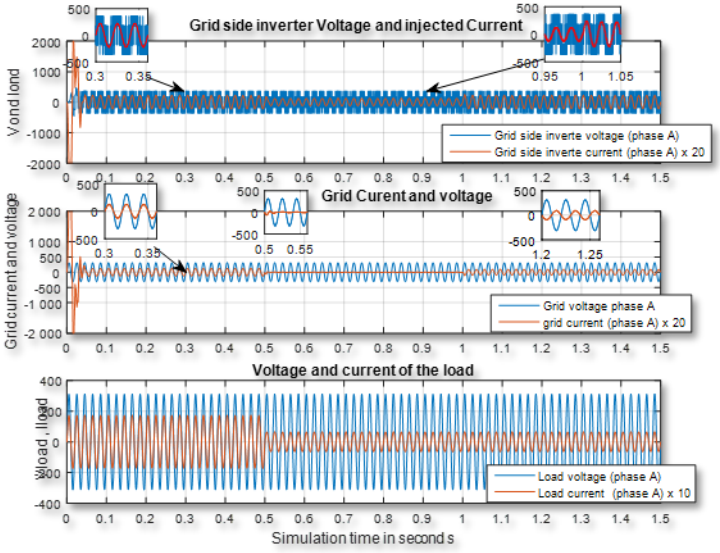

Fig. 19. One-phase voltages and currents of the system

From Figs. 15 (a) and 15(b) we observe that the evolution of the Vpv voltage always tracks the $Vmpp$ voltage, which means the operating point of the panels is maintained at its optimal operating point. Fig. 15 (c) shows a good regulation of the DC link voltage to its desired reference value, using the PI regulator.

Fig. 16 shows the three-phase currents delivered by the system with undistorted sinusoidal form. This gives us a clear view of the power flow of each

element in PVECS. It is clear that the phase of the inverter signals is fixed on the grid estimated frequency, which is the inverse of the period T=0.02s, like shown in figure.

Fig. 18 shows for each component of the system it's power flow in the three different steps of simulation. We can see the contribution of the grid when the demand of the building is higher than the PV generator energy, in reverse when the building has positive energy the grid becomes a receiver, this is justified by the negative sign of the power.

On Fig. 19 we plot the voltage and current of one phase (a) of each element of the PVECS. This figure illustrates clearly the contribution of the grid and the PV generator to supply the building for $t < 0.5\ s$. When the load is changed to 3 kW from $0.5 < t < 1\ s$ and under less irradiance 600 Watt/m² (3.15 kW), we observe that the grid current becomes almost zero and the load demand is satisfied from PVS only. In the third step, when $t > 1\ s$ the solar irradiation has reached G=1000 W/m², therefore the PV generator produce 5.4 kW of electric power. The energy demand of the building is satisfied by the PVS (3kW) and the rest of the generated power is injected into the grid. The opposite of the phase shift between grid current and voltage clearly indicate the injection into the grid and the inverse direction of the power flow.

7. Conclusions

In this work, we presented the modeling and simulation of a photovoltaic system that supplies AC loads of the building and that is connected to the grid. The PV panels were connected with a boost chopper to extract the maximum power. The use of fuzzy MPPT has proven its robustness against disturbances of the loads and climatic changes. Our objective is to fully transfer the generated photovoltaic power to the building and to the grid. We proposed a simple-to-implement control strategy based on maintaining a unity power factor. The PLL controller assures a good synchronization to the grid.

The PI and hysteresis controllers of the AC converter allows us to maintain the energy balance between the building with the grid side and the PVECS. In addition, it leads to the voltage stabilization of the DC-link. In the favorable climatic conditions, the PVECS can alone satisfy the need of the loads (building), and completely replace the contribution of the grid, this will reduce the dependence of traditional fossil energy sources.

R E F E R E N C E S

[1] *L. Bellia, F. De Falco and F. Minichiello*, Effects of solar shading devices on energy requirements of standalone office buildings for Italian climates, Applied Thermal Engineering, 2013, vol. 54, iss. 1, pp. 190-201.

[2] *Stéphane, Thiers,* Bilans énergétiques et environnementaux de bâtiments à énergie positive. PhD Thesis, École Nationale Supérieure des Mines de Paris, 2008.
[3] *Virgil DUMBRAVA, George Cristian LAZAROIU, et al, "*Photovoltaic production management in stochastic optimized microgrids", UPB Scientific Bulletin, Series C: Electrical Engineering, Vol. 79, Iss. 1, 2017, pp. 225-244, ISSN 2286 – 3540.
[4] *T. Alnejaili, S. Drid, D. Mehdi and L. Chrifi-Alaoui,* A Developed energy management strategy for a stand-alone hybrid power system for medium rural health building, the International Transactions on Electrical Energy Systems, Vol. 26, N°. 4, pp.713–729, 2016.
[5] *L. Xu, R. Cheng and J. Yang,* A New MPPT Technique for Fast and Efficient Tracking under Fast Varying Solar Irradiation and Load Resistance, International Journal of Photo energy, vol. 2020, pp. 1-18, 2020.
[6] *J. Kang et al.,* A Novel MPPT Control of photovoltaic system using FLC algorithm, 11th International Conference on Control, Automation and Systems, pp.434-439, 2011.
[7] *H. Yatimi, Y. Ouberri and E. Aroudam,* Enhancement of Power Production of an Autonomous PV System based on robust MPPT technique, Procedia Manufacturing, vol. 32, pp. 397-404, 2019.
[8] *U. Yilmaz, a. Kircay, s. Borekci,* PV system fuzzy logic MPPT method and PI control as a charge controller, Renewable and Sustainable Energy Reviews, vol. 81, pp. 994-1001, 2018.
[9] *N.g.m. Thao, Nguyen, k. Uchida,* A novel fuzzy-based control strategy for grid-connected large-scale solar farm with supporting the grid-frequency regulation, 10th Asian Control Conference (ASCC). IEEE, 2015. pp. 1-8, 2015.
[10] *S. Jain, l. Goyal,* Current control methodology for PV in both standalone & Grid connected mode, IEEE 6th India International Conference on Power Electronics (IICPE). IEEE, pp. 1-7, 2014.
[11] *G. Ramya, R. Ramaprabha, "*Performance analysis of photovoltaic fed grid tied modular multilevel converter*",* UPB Scientific Bulletin, Series C: Electrical Engineering, Vol. 82, Iss. 3, 2020, pp. 195-210, ISSN 2286-3540.
[12] *B. Bendib, h. Belmili, f. Krim,* A survey of the most used MPPT methods: Conventional and advanced algorithms applied for photovoltaic systems, Renewable and Sustainable Energy Reviews, vol. 45, pp. 637-648, 2015.
[13] *Srivastava, Manaswi et Saxena, Apoorva,* Direct and quadrature axis voltage and current control of a three phase grid connected PV system with Adaptive Fuzzy Logic MPPT Controller. In: 2016 IEEE 1st International Conference on Power Electronics, Intelligent Control and Energy Systems (ICPEICES). IEEE, 2016. pp. 1-5.
[14] *O. GERGAUD,* Modélisation énergétique et optimisation économique d'un système de production éolien et photovoltaïque couplé au réseau et associé à un accumulateur, Ph.D dissertation, Ecole Normale Supérieure De Cachan, 2002.
[15] *MM. REFAAT, et al,* Adaptive Fuzzy Logic Controller as MPPT Optimization Technique Applied to Grid-Connected PV Systems. In: Modern Maximum Power Point Tracking Techniques for Photovoltaic Energy Systems, Springer, Cham. pp. 247-281, 2020.
[16] *A. OI,* Design and simulation of photovoltaic water pumping system, Ph.D. dissertation, California Polytechnic State University, 2005.
[17] *C. Cabal,* Optimisation énergétique de l'étage d'adaptation électronique dédié à la conversion photovotaïque, Ph.D. dissertation, University of Toulouse III-Paul Sabatier, 2008.
[18] *Ma. Eltawil, z.zhao,* MPPT techniques for photovoltaic applications, Renewable and sustainable energy reviews, vol. 25, pp. 793-813, 2013.
[19] *S. Vasantharaj, G. Vinodhkumar, M. Sasikumar,* Development of a Fuzzy Logic based, Photovo/taic Maximum Power Point tracking control system using boost converter, lET Chennai 3rd International conference on Sustainable Energy and Intelligent Systems, 2012.
[20] *S.Golzari, F. Rashidi, Hf Farahani,* A Lyapunov function based model predictive control for

three phase grid connected photovoltaic converters, Solar Energy, vol. 181, pp. 222-233, 2019.

[21] *A. Chaoui, JP. gaubert, F. Krim*, Power quality improvement using DPC controlled three-phase shunt active filter, Electric Power Systems Research, vol. 80, no 6, pp. 657-666, 2010.

[22] *M. Abdelkrim, B. Achour, BM. Toufik,* Real time implementation of a fuzzy logic based MPPT controller for grid connected photovoltaic system, International Journal of Renewable Energy Research (IJRER), vol. 5, no 1, pp. 236-244, 2015.